DMD Fast Forward. Published on November 3, 2022 as DOI: 10.1124/dmd.122.001038
This article has not been copyedited and formatted. The final version may differ from this version.

Renal Transporter Alterations in Patients with Chronic Liver Diseases: Nonalcoholic Steatohepatitis, Alcohol-associated, Viral Hepatitis, and Alcohol-Viral Combination

Kayla L. Frost*, Joseph L. Jilek*, Shripad Sinari, Robert R. Klein, Dean Billheimer, Stephen H. Wright, & Nathan J. Cherrington

College of Pharmacy, Department of Pharmacology & Toxicology, University of Arizona, Tucson, AZ, USA (KLF, ADT, JLJ, RGS, NJC)

The University of Arizona Center for Biomedical Informatics & Biostatistics, University of Arizona, Tucson, AZ, USA (SS, ET, DDB)

Banner University Medical Center, Department of Pathology, Tucson, AZ, USA (RRK)

College of Medicine, Department of Physiology, The University of Arizona, Tucson, AZ, USA (SHW)

* Denotes equal contribution

RUNNING TITLE

Renal Transporter Alterations in Liver Disease Patients

Corresponding author: Nathan J. Cherrington, cherring@pharmacy.arizona.edu

1295 N Martin Ave, Tucson, AZ, 85721

(520)-626-0219

Number of text pages: 21

Number of tables: 2

Number of figures: 5

Number of references: 31

Number of words in abstract: 243

Number of words in introduction: 665

Number of words in discussion: 1198

Abbreviations: Adverse drug reaction (ADR), alcohol-associated liver disease (ALD), breast cancer resistance protein (BCRP), chronic liver disease (CLD), copper transporter (CTR), equilibrative nucleoside transporter (ENT), hepatitis C virus (HCV), multidrug and toxin extrusion (MATE), multidrug resistance-associated protein (MRP), multidrug resistance protein (MDR), nonalcoholic fatty liver disease (NAFLD), nonalcoholic steatohepatitis (NASH), organic anion transporter (OAT), organic anion transporting peptides (OATP), organic cation transporters (OCT), organic cation uptake transporter (OCTN), peptide transporter (PEPT), sodium/bile acid cotransporter (NTCP), sodium-glucose cotransporter (SGLT), urate transporter (URAT)

DMD Fast Forward. Published on November 3, 2022 as DOI: 10.1124/dmd.122.001038
This article has not been copyedited and formatted. The final version may differ from this version.

ABSTRACT

Alterations in hepatic transporters have been identified in pre-cirrhotic chronic liver diseases (CLD) that result in pharmacokinetic variations causing adverse drug reactions (ADRs). However, the effect of CLD on the expression of renal transporters is unknown despite the overwhelming evidence of kidney injury in CLD patients. This study determines the transcriptomic and proteomic expression profiles of renal drug transporters in patients with defined CLD etiology. Renal biopsies were obtained from patients with a history of CLD etiologies, including nonalcoholic fatty liver disease (NAFLD), nonalcoholic steatohepatitis (NASH), alcohol-associated liver disease (ALD), viral hepatitis C (HCV), and combination ALD/HCV. A significant decrease in organic anion transporter 3 (OAT3) was identified in NASH, ALD, HCV, and ALD/HCV (1.56± 1.10; 1.01± 0.46; 1.03± 0.43; 0.86± 0.57 pmol/mg protein) relative to control (2.77± 1.39 pmol/mg protein). Additionally, a decrease was shown for OAT4 in NASH (24.9± 5.69 pmol/mg protein) relative to control (43.8± 19.9 pmol/mg protein) and in urate transporter 1 (URAT1) for ALD and HCV (1.56± 0.15 and 1.65± 0.69 pmol/mg protein) relative to control (4.69± 4.59 pmol/mg protein). These decreases in organic anion transporter expression could result in increased and prolonged systemic exposure to drugs and possible toxicity. Renal transporter changes, in addition to hepatic transporter alterations should be considered in dose adjustments for CLD patients for a more accurate disposition profile. It is important to consider a multi-organ approach to altered pharmacokinetics of drugs prescribed to CLD patients to prevent ADRs and improve patient outcomes.

DMD Fast Forward. Published on November 3, 2022 as DOI: 10.1124/dmd.122.001038
This article has not been copyedited and formatted. The final version may differ from this version.

SIGNIFICANCE STATEMENT

Chronic liver diseases are known to elicit alterations in hepatic transporters that result in a disrupted pharmacokinetic profile for various drugs. However, it is unknown if there are alterations in renal transporters during chronic liver disease, despite strong indications of renal dysfunction associated with chronic liver disease. Identifying renal transporter expression changes in patients with chronic liver disease facilitates essential investigations on the multifaceted relationship between liver dysfunction and kidney physiology to offer dose adjustments and prevent adverse drug reactions.

DMD Fast Forward. Published on November 3, 2022 as DOI: 10.1124/dmd.122.001038
This article has not been copyedited and formatted. The final version may differ from this version.

INTRODUCTION

Transporters are well-accepted as essential components of absorption, distribution, metabolism, and elimination (ADME) processes for drugs. Various diseases demonstrate altered function of transporters that lead to the disruption of predicted pharmacokinetic profiles that can result in adverse drug reactions (ADRs) (Evers et al., 2018). This is implicit in the Food and Drug Administration (FDA) requirement to evaluate select transporters in drug-drug interaction studies (FDA, 2022). Since the liver and kidney are considered the primary organs involved in ADME processes, knowing their respective transporter expression and function during disease states is imperative for preventing ADRs (Droździk et al., 2020). Specifically, hepatic transporter alterations in chronic liver diseases (CLD) have been well characterized and are considered when predicting ADRs through shifts in pharmacokinetic profiles (More et al., 2013; Wang et al., 2016; Vildhede et al., 2020). The major forms of CLD include nonalcoholic fatty liver disease (NAFLD) and its progressive form, nonalcoholic steatohepatitis (NASH), alcohol-associated liver disease (ALD), and viral hepatitis C (HCV) (Moon et al., 2020). CLD has an overwhelming global prevalence estimated at 1.5 billion persons in 2017 and a mortality rate of approximately 2 million deaths annually (Moon et al., 2020). While alterations of hepatic transporters and potential pharmacokinetic disruptions are well documented in each of these CLD etiologies, renal transporter expression in CLD patients is largely unknown (More et al., 2013; Wang et al., 2016; Droździk et al., 2020; Vildhede et al., 2020).

Changes in renal pathology of patients with CLD has been observed for decades starting with the documentation of glomerular abnormalities and nephropathy using microscopy (Sakaguchi, 1968; Axelsen et al., 1995). Implementation of the Model of End-Stage Liver Disease (MELD) system in 2002, which includes serum creatinine as a variable, has drastically increased the number of simultaneous liver and kidney transplants (SLKT) by over 200% in the United States (Pita et al., 2019). Despite reports of approximately 25% of patients awaiting liver transplantation (LT) having irreversible kidney damage, only 1-2% of patients receive renal biopsies due to its invasiveness (Wieliczko et al., 2020) (Tsapenko et

DMD Fast Forward. Published on November 3, 2022 as DOI: 10.1124/dmd.122.001038
This article has not been copyedited and formatted. The final version may differ from this version.

al., 2012). As such, this presents a major challenge in investigating renal transporter alterations in patients with CLD due to limited sample availability. Obtaining kidney biopsies from patients with defined liver diseases was a significant advancement given the increasing number of patients receiving SLKT and the substantial number of pharmaceuticals that rely on renal elimination through transporters.

Renally excreted drugs are primarily eliminated through glomerular filtration and active tubular secretion by transporters (Paglialunga et al., 2017). Modifications in either of these processes leads to altered pharmacokinetic responses that could result in ADRs through deviations in the targeted systemic concentration (Matzke et al., 2011; Paglialunga et al., 2017). Renal drug transporters are primarily located in proximal tubule cells and can be categorized as uptake (basolateral or apical) or efflux (basolateral or apical) to comprehensively estimate the distribution of drugs for pharmacokinetic predictions (Nigam et al., 2015). As such, depending on substrate specificity, drugs can be taken into proximal tubule cells by basolateral uptake, effluxed into the lumen by apical efflux, and eliminated in urine. Additionally, drugs can also be taken into the proximal tubule cell from the lumen by apical uptake and effluxed into systemic circulation by basolateral efflux transporters (Nigam et al., 2015). Increases or decreases in transporters controlling these distribution and elimination processes can cause systemic concentrations of drugs to rise above the therapeutic window resulting in toxicity or fall below the therapeutic window resulting in decreased efficacy.

Determining alterations in renal transporters in patients with CLD will allow the prediction of possible pharmacokinetic shifts to prevent ADRs. ADRs in this growing population is a major public health concern, therefore, this study investigates transcriptomic and proteomic expression profiles of renal transporters in patients with common etiologies of CLD to aid in these pharmacokinetic predictions. Identification of renal transporter alterations in patients with CLD have the potential to improve patient outcomes by facilitating future studies that may support dose adjustments in medications to prevent potential ADRs.

DMD Fast Forward. Published on November 3, 2022 as DOI: 10.1124/dmd.122.001038
This article has not been copyedited and formatted. The final version may differ from this version.

METHODS

Renal Biopsies

Renal biopsies were obtained from Banner University Medical Center as previously described by Frost *et al*. (Frost et al., 2022). In brief, medical charts of all patients with available renal biopsies that contained International Classification of Disease 9 and 10 codes (ICD9, ICD10) for liver pathology were identified. Characterization of liver and kidney pathology and social histories were recorded upon chart review in Epic Hyperspace healthcare system. Following exclusion criteria described previously, patients were determined as NAFLD (n = 6), NASH (n = 5), ALD (n = 6), HCV (n = 6), or ALD/HCV (n = 6). Control patients (n = 7) were uniquely classified throughout the chart review process and deemed normal upon renal pathology and abdominal imaging assessment. Demographics and biochemical function tests are available in previously published materials (Frost et al., 2022) and briefly summarized in Table 1. Samples obtained and patient information documented are in accordance with Institutional Review Board (IRB) approval.

Transcriptomics

Transcriptional expression was determined by Affymetrix Clariom D arrays according to published protocols established by Affymetrix. Detailed methods of RNA isolation and microarray expression profiling were previously published by Frost *et al. (Frost et al., 2022).* In summary, formalin-fixed paraffin-embedded (FFPE) renal needle biopsy specimens were gouged, and half of the sample proceeded with RNA isolation and quality control checks. Following isolation, genome wide expression profiling was determined using arrays with more than 28,000 gene-level probe sets. GeneChip Expression Console (Affymetrix, Santa Clara, CA) was used to analyze the stained arrays and generate cell intensity data. The cell intensity data were analyzed using the robust multiarray average method (RMA) and reported as background-adjusted, normalized, and log-transformed expression (Irizarry et al., 2003).

Quantitative Protein Expression

DMD Fast Forward. Published on November 3, 2022 as DOI: 10.1124/dmd.122.001038
This article has not been copyedited and formatted. The final version may differ from this version.

The remaining half of the gouged FFPE renal biopsy was deparaffinized and hydrated prior to heat-induced antigen retrieval (HIAR) as previously published (Frost et al., 2022). Of the 36 specimens, two biopsies did not have enough tissue leftover from transcriptomics to proceed with protein processing and were excluded from analysis (1 ALD and 1 ALD/HCV). To achieve HIAR, samples were ultrasonicated and boiled in 80 µL of HIAR buffer (100 mmol/L Tris-HCl [pH 8.5], 100 mmol/L dithiothreitol (DTT), and 4% SDS) (Sigma—Aldrich, St. Louis, MO). Protein was precipitated with 500 µL of cold methanol, 100 µL chloroform, and 400 µL of water and centrifuged for 1-minute at 16,000 X *g*. After removing the solvent and washing the pellet with methanol, the pellet was dissolved in 100 µL of buffer (100 mmol/L ammonium bicarbonate (Oakwood Chemical, Estill, SC) and 3.7% sodium deoxycholate (Sigma—Aldrich, St. Louis, MO) before measuring total protein with a Pierce™ Protein BCA Assay Kit. The protein precipitate was denatured, alkylated, and quenched prior to trypsin digestion with Pierce™ Trypsin/Lys-C at a 1:25 enzyme to substrate ratio. The trypsin digestion was quenched with 0.4% formic acid containing a heavy isotope labeled amino acid ($^{13}C/^{16}N$) internal standard cocktail **(Table 2)**. Strong cation exchange columns (Waters, Inc., Milford, MA) were used according to the manufacture's protocol, and peptides were eluted by 200 µL of 60:40 water: acetonitrile (ACN) with 2% ammonium hydroxide followed by 200 µL of ACN with 2% ammonium hydroxide. The eluent was dried down and reconstituted in 40 µL of 5% mobile phase (95:5 water: ACN with 0.1% formic acid).

Liquid chromatography-coupled mass spectrometry (LC-MS/MS) instrumental parameters for surrogate peptide quantification are consistent with previously published methods, apart from injection volume, which was increased to 10 µL (Frost et al., 2022). A binary solvent gradient (water + 0.1% formic acid aqueous; 90:10 ACN: water with 0.1% formic acid organic) was run on an Agilent UPLC system using a Acquity UPLC® HSS C18 column (2.1 mm X 100 mm) with 1.8 µm particles (Waters, Inc.). Peptides were detected with a Sciex QTrap 6500+ mass spectrometer operated in positive mode with electrospray ionization (ESI) and multiple reaction monitoring (MRM), with respective transitions identified in **Table 2**. Relative protein expression was quantified by Analyst MultiQuant (version 3,

DMD Fast Forward. Published on November 3, 2022 as DOI: 10.1124/dmd.122.001038
This article has not been copyedited and formatted. The final version may differ from this version.

Sciex) according to calibration range and heavy-labeled internal standard peptides, and total protein abundance was calculated by adjusting for percent yield upon peptide digestion and elution as described by Jilek *et al*. (Jilek et al., 2021). The total protein abundance reported is relative to these preserved samples and the differences in protein expression reported are relative to controls samples preserved and processed by the same techniques.

Statistics

Data was graphed and analyzed using GraphPad Prism 9.0 software and is represented as mean ± standard deviation. Cell intensity data for transcriptional analysis are analyzed by the robust multiarray average method (RMA) and reported as background-adjusted, normalized, and log-transformed expression with relative mean comparisons to the mean of control samples (Irizarry et al., 2003). For transcriptional expression, unadjusted p-values ≤ 0.05 are reported as differential expression given the small sample size and patient variability. For protein expression, the mean of each disease group was independently compared to the mean of the control group using a one-way analysis of variance with Fisher's Least Significant Differences test to determine statistical significance defined as $p \leq 0.05$. All samples were included in statistical analyses regardless of outlier tests due to small sample size. Samples were only excluded from protein expression analysis if there was not enough protein to quantify, as determined using BCA.

RESULTS

Transcriptional Expression

Affymetrix microarrays were used for genome wide expression profiling and gene expression for relevant transporters were examined. Normalized gene expression for relevant renal uptake and efflux transporters are graphed in **Figure 1**. Patient variability, limited sample size in each disease group, small needle biopsy tissue amount, and the intense preservation of FFPE are taken into consideration when evaluating statistical significance of changes in disease groups relative to control. As such, unadjusted p-

DMD Fast Forward. Published on November 3, 2022 as DOI: 10.1124/dmd.122.001038
This article has not been copyedited and formatted. The final version may differ from this version.

values of less than or equal to 0.05 were considered as differential expression. For the uptake transporters, decreases were observed for sodium/bile acid cotransporter (SLC10A1; NTCP) in NASH (-0.5), ALD (-0.4), and HCV (-0.5) and for sodium/nucleoside cotransporter 1 (SLC28A1; CNT1) in ALD/HCV (-0.4) with a mean $\log_2$ fold-change relative to control. The mean $\log_2$ fold-change relative to control increased for organic anion transporter 4 (SLC22A11; OAT4) in ALD (0.4) and sodium-dependent phosphate transporter 4 (SLC17A3; NPT4) in HCV (1.2) and ALD/HCV (1.4) **(Figure 1A)**. However, the mean $\log_2$ fold-change relative to control increased for a few efflux transporters including, P-glycoprotein (ABCB1; P-gp) in NASH (0.5) and HCV (0.5); multidrug resistance-associated protein 3 (ABCC3; MRP3) in ALD/HCV (1.0); and MRP4 (ABCC4) in HCV (0.8) (**Figure 1B)**.

Protein Expression of Uptake Transporters

Surrogate peptides were used to quantify protein expression of organic anion and cation transporters using LC-MS/MS. All disease groups, except NAFLD, demonstrated a significant decrease in OAT3 expression (NASH 1.56 ± 1.10; ALD 1.01 ± 0.46; HCV 1.03 ± 0.43; ALD/HCV 0.86 ± 0.57 pmol/mg protein) relative to control (2.77 ± 1.39 pmol/mg protein). NASH, additionally, showed decreased expression for OAT4 (24.9 ± 5.69 pmol/mg protein) and OAT7 (0.05 ± 0.03 pmol/mg protein) relative to control (43.8 ± 19.9 and 0.12 ± 0.07 pmol/mg protein, respectively). ALD and ALD/HCV, however, showed decreased expression for urate transporter 1 (URAT1; 1.56 ± 0.15 and 1.65 ± 0.69 pmol/mg protein) relative to control (4.69 ± 4.59 pmol/mg protein). The only significant increases in expression observed for organic anion transporters were in the NAFLD group for OAT2 (1.08 ± 1.14 pmol/mg protein) and OATP1A2 (0.85 ± 0.85 pmol/mg protein) relative to control (0.40 ± 0.38 and 0.24 ± 0.19 pmol/mg protein, respectively) **(Figure 2)**. Similarly, the only increase observed for organic cation transporters was also in the NAFLD group for carnitine/organic cation transporter 2 (OCTN2) (2.62 ± 2.97 pmol/mg protein) and multidrug and toxin extrusion protein 2 (MATE2-K) (3.90 ± 2.99 pmol/mg protein) relative to control (0.85 ± 0.92 and 0.94 ± 0.37 pmol/mg protein, respectively) **(Figure 3)**.

DMD Fast Forward. Published on November 3, 2022 as DOI: 10.1124/dmd.122.001038
This article has not been copyedited and formatted. The final version may differ from this version.

Protein Expression of Efflux and Additional Relevant Transporters

Renal efflux and other relevant transporters were quantified by surrogate peptide LC-MS/MS after trypsin digestion. None of the disease groups, except NAFLD, demonstrated a significant increase relative to control for the ATP-binding cassette (ABC) efflux transporters. NAFLD was increased for MRP1 (5.21 ± 5.66 pmol/mg protein) and breast cancer resistance protein (BCRP) (0.98 ± 0.57 pmol/mg protein) relative to control (1.60 ± 1.20 and 0.39 ± 0.31 pmol/mg protein, respectively). P-gp expression for ALD (1.53 ± 0.31 pmol/mg protein) relative to control (2.58 ± 1.24 pmol/mg protein) was the only observed decreased for ABC efflux transporters **(Figure 4)**.

Protein expression of equilibrative nucleoside transporters (ENT1-2) and sodium/nucleoside cotransporters (CNT1-3) were also quantitated. NAFLD and NASH showed a decrease in ENT1 (21.1 ± 13.7 and 22.2 ± 9.20 pmol/mg protein, respectively) compared to control (44.2 ± 15.0 pmol/mg protein). However, NAFLD showed an increase in CNT2 (1.67 ± 1.53 pmol/mg protein) while NASH and ALD showed an increase in CNT1 (44.7 ± 25.2 and 39.2 ± 23.8 pmol/mg protein, respectively) relative to control (0.51 ± 0.42 and 19.1 ± 8.17 pmol/mg protein, respectively) **(Figure 5a)**. Sodium/glucose cotransporter (SGLT2) and peptide transporters (PEPT1-2) were also quantified but did not demonstrate any changes apart from the widely variable NASH increase for PEPT1 (107 ± 126 pmol/mg protein) relative to control (20.7 ± 20.6 pmol/mg protein) **(Figure 5b)**. Bile acid transporters, ileal sodium/bile acid cotransporter (ASBT), NTCP, and organic solute transporter (OSTα-β) were quantified but demonstrated no significant changes for any of the liver disease groups **(Figure 5c)**.

DISCUSSION

Transporters are critical components of ADME properties for drugs and are particularly instrumental for drugs that rely on hepatic and renal elimination. Alterations in hepatic and renal transporters can cause shifts in predicted pharmacokinetic profiles of drugs leading to unknown ADRs. Shifts in pharmacokinetic profiles due to hepatic transporter alterations have been demonstrated in

DMD Fast Forward. Published on November 3, 2022 as DOI: 10.1124/dmd.122.001038
This article has not been copyedited and formatted. The final version may differ from this version.

various CLD studies for a multitude of compounds. Observations of a general decrease in hepatic basolateral uptake and canalicular efflux transporters in NASH, ALD, and HCV suggest an increase in plasma retention and decrease in biliary excretion of drugs with substrate specificity for these altered transporters (More et al., 2013; Wang et al., 2016; Vildhede et al., 2020). This results in higher systemic concentrations and prolonged exposure to drugs than what is predicted in standard toxicity screens for FDA approval. Although there have been several investigations of hepatic transporter alterations in CLD patients, resulting in the identification of dosing adjustments, there is nothing known regarding alterations of renal transporters in these patients (Droździk et al., 2020). The shortage of information is multifactorial, but the primary limitations include discrepancies in diagnosing CLD etiology, inaccuracy of kidney function assays to indicate renal biopsy evaluation, and invasiveness of biopsy procedures (Beben and Rifkin, 2015; Porrini et al., 2019; Younossi et al., 2019; Wieliczko et al., 2020; Lai et al., 2021). Combined, these limitations hinder clinical studies by restricting sample availability. This is the first clinical study to overcome this limitation and determine the expression of renal transporters in patients with defined CLD etiologies. The changes identified in this study will aid potential dose adjustment recommendations to prevent ADRs and ensure therapeutic efficacy in this growing population.

Alterations in organic anion transporters (OATs) contribute to pharmacokinetic variability through their critical role in ADME processes for a broad range of clinically relevant drugs, including nonsteroidal anti-inflammatory (NSAIDs), diuretics, anti-hypertensives, and antivirals (Emami Riedmaier et al., 2012; Zhang et al., 2021). OATs are expressed at the basolateral (OAT1-3) and apical (OAT4 and URAT1) membranes of proximal tubule cells and participate in both elimination and reabsorption of compounds (Zhang et al., 2021). OATs are not only critical for the homeostasis of endogenous compounds and metabolites, but have been identified as a major contributor to renal secretion processes for a variety of compounds, with OAT3 proposed as the major contributor to basal uptake (Mathialagan et al., 2017). As such, the decrease in protein expression observed in OAT3 for NASH, ALD, HCV, and

DMD Fast Forward. Published on November 3, 2022 as DOI: 10.1124/dmd.122.001038
This article has not been copyedited and formatted. The final version may differ from this version.

ALD/HCV is of major concern for evaluating ADRs in these patients. A decrease in OAT3 could lead to diminished uptake of drugs for renal excretion, resulting in higher systemic exposure concentrations. Drug-drug interaction studies supported this concept through co-administration of OAT3 inhibitor lansoprazole with pemetrexed in non-small cell lung cancer patients that lead to hematologic toxicity caused by decreased uptake and elimination of pemetrexed (Ikemura et al., 2016).

In addition to considering renal transporter alterations for predictions in pharmacokinetics, the initial change in drug disposition resulting from hepatic transporter alterations in liver disease etiology must also be considered. This complexity can be evaluated by considering the pharmacokinetic alterations of methotrexate in NASH. Methotrexate is taken into hepatocytes by the basolateral uptake transporter OATP1B3 and effluxed back into systemic circulation by MRP3 or excreted into bile by canalicular efflux transporter MRP2 (Hardwick et al., 2014). In NASH, however, a decrease in hepatic OATP1B1 and increase in MRP3 protein expression, and functional decrease in MRP2 due to mislocalization, leads to an increase in plasma concentrations of methotrexate (Hardwick et al., 2014; Vildhede et al., 2020). Adding to this concern for increased systemic concentrations of methotrexate, is that methotrexate can be renally eliminated by basolateral uptake through OAT3, which is shown in this study to be decreased in NASH patients (Chioukh et al., 2014). As such, the increase in systemic concentration of methotrexate observed in NASH may be attributed to the decrease of renal OAT3 in addition to the alteration in hepatic transporters. This demonstrates a concern for physiologically based pharmacokinetic (PBPK) models that only consider hepatic transporter alterations for predicting pharmacokinetic profile disposition. Therefore, these results are intended to inform PBPK models of the possible changes in renal elimination when evaluating potential ADRs in these chronic liver disease populations. A previous application of this concept was demonstrated by the improvement of predicting repaglinide altered disposition in liver cirrhosis patients when incorporating the alteration of hepatic OATP1B1 in the PBPK module (Wang et al., 2016). Therefore, to expand the predictive power of PBPK modeling for drug disposition, these results could be implemented for additional pharmacokinetic profile disruptions with the respective renal

DMD Fast Forward. Published on November 3, 2022 as DOI: 10.1124/dmd.122.001038
This article has not been copyedited and formatted. The final version may differ from this version.

transporters identified. It is imperative that the dose adjustment in these patients not only consider the effect caused by hepatic transporter alterations on pharmacokinetic variations, but the renal transporters as well to prevent unwarranted ADRs.

The importance of taking specific liver disease etiology into consideration for dose adjustments is exemplified by the differential changes to apical organic anion transporters by disease. A decrease in OAT4 was only demonstrated in NASH while a decrease in URAT1 was only demonstrated in ALD and HCV. This demonstrates that etiology should be considered when estimating pharmacokinetic alterations to assure achievement of therapeutic concentrations, as well as proposing fundamental differences in the mechanism of altered renal secretory physiology associated with each CLD etiology. For example, lowering the dose of zidovudine (AZT), an antiviral used for the treatment of HIV that can cause hematotoxicity, might be considered for a patient with NASH since it is a substrate of OAT3 and OAT4 (Langtry and Campoli-Richards, 1989; Takeda et al., 2002). However, the dose may need to be decreased further to prevent toxicity for patients with ALD or HCV because they display decreased OAT3 but normal OAT4, which may result in reabsorption of AZT. While there are no known drugs that are substrates for URAT1, the decrease shown in ALD and HCV could have substantial impacts on physiological homeostasis for uric acids and uricosuric drugs (Lozano et al., 2018).

Although this innovative clinical study overcomes extensive challenges to obtain a cohort of renal biopsy samples from patients with verified liver pathology for expressional characterization, the restricted sample size remains a primary limitation for defining transporter abundance variability. As such, the frequency of each liver disease with altered transporter function is an association and cannot be concluded as an explicit relationship (Frost et al., 2022). However, this investigation emphasizes the criticality of future analyses into the relationship between chronic liver diseases and associated renal dysfunction in the context of ADR prevention. The quantification of altered expression of the renal organic anion transporters reported here in patients with NASH, ALD, HCV, and ALD/HCV should assist future studies that investigate potential pharmacokinetic variations of clinically relevant drugs to prevent ADRs. This

DMD Fast Forward. Published on November 3, 2022 as DOI: 10.1124/dmd.122.001038
This article has not been copyedited and formatted. The final version may differ from this version.

study represents the first identification of expression profiles of renal drug transporters in patients with pre-cirrhotic CLD etiologies and will be instrumental in moving forward with mechanistic studies. Understanding the prospective pharmacokinetic profile shifts in this growing population is vital for improving patient outcomes. It is imperative that these changes continue to be investigated through pre-clinical models and clinical trials to enable dose adjustments that will prevent ADRs and ensure patient safety.

DMD Fast Forward. Published on November 3, 2022 as DOI: 10.1124/dmd.122.001038
This article has not been copyedited and formatted. The final version may differ from this version.

ACKNOWLEDGEMENTS

The authors would like to thank Jim Galligan, PhD, and Erin Jennings for consulting on the method development for surrogate peptide quantification.

AUTHOR CONTRIBUTIONS

Participated in research design: Frost, Jilek, Klein, Wright, and Cherrington

Conducted experiments: Frost and Jilek

Contributed new reagents or analytical tools: Frost, Jilek, Sinari, Billheimer, and Cherrington

Performed data analysis: Frost, Jilek, Sinari, Billheimer, Wright, and Cherrington

Wrote or contributed to the writing of the manuscript: Frost, Jilek, and Cherrington

DMD Fast Forward. Published on November 3, 2022 as DOI: 10.1124/dmd.122.001038
This article has not been copyedited and formatted. The final version may differ from this version.

REFERENCES

Axelsen RA, Crawford DH, Endre ZH, Lynch SV, Balderson GA, Strong RW, and Fleming SJ (1995) Renal glomerular lesions in unselected patients with cirrhosis undergoing orthotopic liver transplantation. *Pathology* **27:**237-246.

Beben T and Rifkin DE (2015) GFR Estimating Equations and Liver Disease. *Adv Chronic Kidney Dis* **22:**337-342.

Chioukh R, Noel-Hudson MS, Ribes S, Fournier N, Becquemont L, and Verstuyft C (2014) Proton pump inhibitors inhibit methotrexate transport by renal basolateral organic anion transporter hOAT3. *Drug Metab Dispos* **42:**2041-2048.

Droździk M, Oswald S, and Droździk A (2020) Extrahepatic Drug Transporters in Liver Failure: Focus on Kidney and Gastrointestinal Tract. *Int J Mol Sci* **21**.

Emami Riedmaier A, Nies AT, Schaeffeler E, and Schwab M (2012) Organic anion transporters and their implications in pharmacotherapy. *Pharmacol Rev* **64:**421-449.

Evers R, Piquette-Miller M, Polli JW, Russel FGM, Sprowl JA, Tohyama K, Ware JA, de Wildt SN, Xie W, and Brouwer KLR (2018) Disease-Associated Changes in Drug Transporters May Impact the Pharmacokinetics and/or Toxicity of Drugs: A White Paper From the International Transporter Consortium. *Clin Pharmacol Ther* **104:**900-915.

FDA (2022) In Vitro Drug Interaction Studies—Cytochrome P450 Enzyme- and Transporter-Mediated Drug Interactions Guidance for Industry, U.S. Department of Health and Human Services Food and Drug Administration Center for Drug Evaluation and Research. .

Frost KL, Jilek JL, Thompson AD, Klein RR, Sinari S, Torabzedehkorasani E, Billheimer DD, Schnellmann RG, and Cherrington NJ (2022) Increased Renal Expression of Complement Components in Patients With Liver Diseases: Nonalcoholic Steatohepatitis, Alcohol-Associated, Viral Hepatitis, and Alcohol-Viral Combination. *Toxicol Sci* **189:**62-72.

Hardwick RN, Clarke JD, Lake AD, Canet MJ, Anumol T, Street SM, Merrell MD, Goedken MJ, Snyder SA, and Cherrington NJ (2014) Increased susceptibility to methotrexate-induced toxicity in nonalcoholic steatohepatitis. *Toxicol Sci* **142:**45-55.

Ikemura K, Hamada Y, Kaya C, Enokiya T, Muraki Y, Nakahara H, Fujimoto H, Kobayashi T, Iwamoto T, and Okuda M (2016) Lansoprazole Exacerbates Pemetrexed-Mediated Hematologic Toxicity by Competitive Inhibition of Renal Basolateral Human Organic Anion Transporter 3. *Drug Metab Dispos* **44:**1543-1549.

Irizarry RA, Hobbs B, Collin F, Beazer-Barclay YD, Antonellis KJ, Scherf U, and Speed TP (2003) Exploration, normalization, and summaries of high density oligonucleotide array probe level data. *Biostatistics* **4:**249-264.

Jilek JL, Frost KL, Jacobus KA, He W, Toth EL, Goedken M, and Cherrington NJ (2021) Altered cisplatin pharmacokinetics during nonalcoholic steatohepatitis contributes to reduced nephrotoxicity. *Acta Pharmaceutica Sinica B.*

Lai J, Wang HL, Zhang X, Wang H, and Liu X (2021) Pathologic Diagnosis of Nonalcoholic Fatty Liver Disease. *Arch Pathol Lab Med*.

Langtry HD and Campoli-Richards DM (1989) Zidovudine. A review of its pharmacodynamic and pharmacokinetic properties, and therapeutic efficacy. *Drugs* **37:**408-450.

Lozano E, Briz O, Macias RIR, Serrano MA, Marin JJG, and Herraez E (2018) Genetic Heterogeneity of SLC22 Family of Transporters in Drug Disposition. *J Pers Med* **8**.

Mathialagan S, Piotrowski MA, Tess DA, Feng B, Litchfield J, and Varma MV (2017) Quantitative Prediction of Human Renal Clearance and Drug-Drug Interactions of Organic Anion Transporter Substrates Using In Vitro Transport Data: A Relative Activity Factor Approach. *Drug Metab Dispos* **45:**409-417.

Matzke GR, Aronoff GR, Atkinson AJ, Jr., Bennett WM, Decker BS, Eckardt KU, Golper T, Grabe DW, Kasiske B, Keller F, Kielstein JT, Mehta R, Mueller BA, Pasko DA, Schaefer F, Sica DA, Inker LA, Umans JG, and Murray P (2011) Drug dosing consideration in patients with acute and chronic kidney disease-a clinical update from Kidney Disease: Improving Global Outcomes (KDIGO). *Kidney Int* **80:**1122-1137.

Moon AM, Singal AG, and Tapper EB (2020) Contemporary Epidemiology of Chronic Liver Disease and Cirrhosis. *Clin Gastroenterol Hepatol* **18:**2650-2666.

More VR, Cheng Q, Donepudi AC, Buckley DB, Lu ZJ, Cherrington NJ, and Slitt AL (2013) Alcohol cirrhosis alters nuclear receptor and drug transporter expression in human liver. *Drug Metab Dispos* **41:**1148-1155.

Nigam SK, Wu W, Bush KT, Hoenig MP, Blantz RC, and Bhatnagar V (2015) Handling of Drugs, Metabolites, and Uremic Toxins by Kidney Proximal Tubule Drug Transporters. *Clin J Am Soc Nephrol* **10:**2039-2049.

Paglialunga S, Offman E, Ichhpurani N, Marbury TC, and Morimoto BH (2017) Update and trends on pharmacokinetic studies in patients with impaired renal function: practical insight into application of the FDA and EMA guidelines. *Expert Rev Clin Pharmacol* **10:**273-283.

Pita A, Kaur N, Emamaullee J, Lo M, Nguyen B, Sabour A, Tristan V, Nadim M, Genyk Y, and Sher L (2019) Outcomes of Liver Transplantation in Patients on Renal Replacement Therapy: Considerations for Simultaneous Liver Kidney Transplantation Versus Safety Net. *Transplant Direct* **5:**e490.

Porrini E, Ruggenenti P, Luis-Lima S, Carrara F, Jiménez A, de Vries APJ, Torres A, Gaspari F, and Remuzzi G (2019) Estimated GFR: time for a critical appraisal. *Nat Rev Nephrol* **15:**177-190.

Sakaguchi H (1968) Hepatic glomerulosclerosis--light microscopic study of autopsy cases. *Acta Pathol Jpn* **18:**407-415.

Takeda M, Khamdang S, Narikawa S, Kimura H, Kobayashi Y, Yamamoto T, Cha SH, Sekine T, and Endou H (2002) Human organic anion transporters and human organic cation transporters mediate renal antiviral transport. *J Pharmacol Exp Ther* **300:**918-924.

Tsapenko M, El-Zoghby ZM, and Sethi S (2012) Renal histological lesions and outcome in liver transplant recipients. *Clin Transplant* **26:**E48-54.

Vildhede A, Kimoto E, Pelis RM, Rodrigues AD, and Varma MVS (2020) Quantitative Proteomics and Mechanistic Modeling of Transporter-Mediated Disposition in Nonalcoholic Fatty Liver Disease. *Clin Pharmacol Ther* **107:**1128-1137.

Wang L, Collins C, Kelly EJ, Chu X, Ray AS, Salphati L, Xiao G, Lee C, Lai Y, Liao M, Mathias A, Evers R, Humphreys W, Hop CE, Kumer SC, and Unadkat JD (2016) Transporter Expression in Liver Tissue from Subjects with Alcoholic or Hepatitis C Cirrhosis Quantified by Targeted Quantitative Proteomics. *Drug Metab Dispos* **44:**1752-1758.

Wieliczko M, Ołdakowska-Jedynak U, and Małyszko J (2020) Clinical Relevance of Kidney Biopsy in Patients Qualified for Liver Transplantation and After This Procedure in the Model for End-stage Liver Disease (MELD) Era: Where Are We Today? *Ann Transplant* **25:**e925891.

Younossi ZM, Marchesini G, Pinto-Cortez H, and Petta S (2019) Epidemiology of Nonalcoholic Fatty Liver Disease and Nonalcoholic Steatohepatitis: Implications for Liver Transplantation. *Transplantation* **103:**22-27.

Zhang J, Wang H, Fan Y, Yu Z, and You G (2021) Regulation of organic anion transporters: Role in physiology, pathophysiology, and drug elimination. *Pharmacol Ther* **217:**107647.

FUNDING: This work was funded by the National Institutes of Environmental Health Sciences grants R01ES028668 and P30ES006694.

CONFLICT OF INTEREST: No author has an actual or perceived conflict of interest with the contents of this article.

DMD Fast Forward. Published on November 3, 2022 as DOI: 10.1124/dmd.122.001038
This article has not been copyedited and formatted. The final version may differ from this version.

FIGURE LEGENDS

Figure 1. *Transcriptomic Expression of Transporters.* Gene expression of renal **(A)** uptake and **(B)** efflux transporters from Affymetrix gene array data. Differential expression determined by unadjusted p-values < 0.05 upon normalization indicated by asterisk relative to control group. **A)** A decrease was observed for SLC10A1 (NTCP) in NASH, ALD, and HCV (p = 0.016, 0.009, 0.005, respectively) and for SLC28A1 (CNT1) in ALD/HCV (p = 0.031). Increases were observed for SLC17A3 (NPT4) in HCV and ALD/HCV (p = 0.049 and 0.021, respectively) and SLC22A11 (OAT4) in ALD (p = 0.028). There were no transcriptional changes in uptake transporters for NAFLD. **B)** Increases observed in ABCB1 (P-gp) for NASH and HCV (p = 0.018 and 0.041, respectively); ABCC3 (MRP3) for ALD/HCV (p = 0.047); and ABCC4 (MRP4) for HCV (p = 0.016). There were no changes in transcriptional expression for efflux transporters in NAFLD or ALD.

Figure 2. *Quantitative Protein Expression of Organic Anion Transporters.* Surrogate peptide LC-MS/MS was used to quantitate protein expression of organic anion transporters. All disease groups, except NAFLD, significantly decreased for OAT3. NASH additionally decreased for OAT4 and OAT7. ALD and ALD/HCV also decreased for URAT1. The increases in OAT2 and OATP1A2 for NAFLD are the only transporters significantly changed for NAFLD and are also the only increases observed across all disease groups for organic anion transporters. Changes with statistical significance between disease and control are defined as $p \leq 0.05$ and indicated by an asterisk.

Figure 3. *Quantitative Protein Expression of Organic Cation Transporters.* Protein expression of organic cation transporters was quantitated using surrogate peptide LC-MS/MS. The only observed significant changes occurred in NAFLD and included increases in OCTN2 and MATE2-K. Statistical significance is defined as $p \leq 0.05$ for changes between control and disease and indicated by an asterisk.

Figure 4. *Quantitative Protein Expression of ATP-binding Cassette (ABC) Transporters.* NAFLD demonstrated the only significant increase for ABC transporters which include MRP1 and BCRP. ALD

DMD Fast Forward. Published on November 3, 2022 as DOI: 10.1124/dmd.122.001038
This article has not been copyedited and formatted. The final version may differ from this version.

showed the only other significant change with a decrease in P-gp. Asterisks indicate statistically significant changes relative to control with a p-value ≤ 0.05.

Figure 5. *Quantitative Protein Expression of Additional Transporters.* **A)** Nucleoside transporters, **B)** other relevant transporters, and **C)** bile-acid transporters are quantified by surrogate peptide LC-MS/MS for protein expression changes. Changes in disease relative to control are considered statistically significant with $p \leq 0.05$ and indicated with an asterisk. **A)** ENT1 was decreased for NAFLD and NASH. However, CNT1 was increased for NASH and ALD and CNT2 for NAFLD. **B)** PEPT1 showed an increase for NASH relative to control. **C)** None of the bile-acid transporters significantly changed for the disease groups relative to control.

Table 1. *Summarized Demographics and Clinical Observations.*

	Control (*n* = 7)	NAFLD (*n* = 6)	NASH (*n* = 5)	ALD (*n* = 6)	HCV (*n* = 6)	ALD/HCV (*n* = 6)
Age (mean ± SD)	35.4 ± 19.4	45 ± 20.9	54.2 ± 17.3*	46.2 ± 10.7	57 ± 4.8%*	55.7 ± 6.3*
% Male	57	50	80	33	66	50
% Hispanic or Latino	14	16	40	33	50%	50
% Diabetic	0	33	60	60	66%	66
BMI (mean ± SD kg/m^2)	23.8 ± 3.2	35.4 ± 3.6*	33.6 ± 2.9*	29.7 ± 5.0*	26.3 ± 4.9	27.8 ± 2.1*
GFR (mean ± SD)	78.6 ± 55.9	36.7 ± 21.4*	32.7 ± 15.0*	16.0 ± 11.0*	27.6 ± 11.5*	21.0 ± 11.2*

A summary of demographics and clinical observations of each disease group adapted from the detailed characterizations published in Frost et al., 2022. Mean ± standard deviation or percent of liver disease etiology. Asterisks indicate significant statistical differences relative to control ($p \leq 0.05$).

Table 2. *Surrogate Peptide Transitions.*

Protein	Peptide Sequence	IS	RT (min)	Q1 (Da)	Q3 (Da)
OAT1	TSLAVLGK	BCRP-H	14.2	394.7	487.3
OAT2	LLVYLSVR	SGLT2-H	19.8	481.8	736.4
OAT3	FITILSLSYLGR	MRP4-H	26	691.9	795.4
OAT4	AELFPTPVR	MRP2-H	18	515.3	568.9

DMD Fast Forward. Published on November 3, 2022 as DOI: 10.1124/dmd.122.001038
This article has not been copyedited and formatted. The final version may differ from this version.

OAT7	DTLTLEILK	BCRP-H	20.9	523.3	716.5
OATP1A2	IYDSTTFR	MRP4-H	12.8	501.7	726.3
OATP4C1	DFPAALK	MRP4-H	14.9	381.2	499.3
URAT1	SIFTSTIVAK	BCRP-H	17.7	533.8	866.5
Na/K ATPase	AAVPDAVGK	SGLT2-H	9.1	414.2	586.3
OCT1	LSPSFADLFR	MRP4-H	23.5	576.8	952.5
OCT2	SLPASLQR	OCT2-H	12.1	436.3	671.4
OCT3	TTVATLGR	OCT2-H	10.4	409.7	616.4
OCTN1	AFILDLFR	SGLT2-H	25.9	497.8	776.5
OCTN2	NHTVPLR	SGLT2-H	7.6	418.7	585.4
MATE1	GGPEATLEVR	SGLT2-H	12.8	514.8	516.3
MATE2-K	YLQNQK	MATE2-K-H	4.9	397.2	630.4
MRP1	TPSGNLVNR	OCT2-H	9.3	479.3	759.4
MRP2	GINLSGGQK	MRP2-H	9.9	437.2	589.3
MRP3	QGELQLLR	BCRP-H	16.6	478.8	529.3
MRP4	APVLFFDR	MRP4-H	20.5	482.8	697.4
MRP5	TLSLEAPAR	BCRP-H	13.7	479.3	743.4
BCRP	ENLQFSAALR	BCRP-H	17	574.8	664.4
P-gp	IATEAIENFR	BCRP-H	16	582.3	749.4
ENT1	IPQSVR	BCRP-H	7.5	350.2	489.3
ENT2	LAGAGNSTAR	OCT2-H	4.8	459.2	733.4
CNT1	LVYPEVEESK	BCRP-H	14.1	596.8	980.5
CNT2	EVEPEGSK	BCRP-H	3.8	437.7	517.3
CNT3	DIASGAVR	BCRP-H	2.3	301.7	414.2
SGLT2	GTVGGYFLAGR	SGLT2-H	17.6	549.3	840.4
PEPT1	DGLNQKPEK	OCT2-H	5	514.8	856.5
PEPT2	IEDIPANK	BCRP-H	9.7	450.2	657.4
ASBT	FLGHIK	SGLT2-H	10.6	357.7	454.3
NTCP	GIYDGDLK	BCRP-H	13.1	440.7	710.3
OSTα	YTADLLEVLK	BCRP-H	22.2	582.8	900.5
OSTβ	DHNSLNNLR	BCRP-H	9.8	541.8	629.4
BCRP-H	ENLQFSA*ALR		17	576.9	668.4
MRP2-H	GINL*SGGQK		9.9	440.7	710.4
MRP4-H	APVL*FFDR		20.5	486.3	704.4
OAT1-H	TSLA*VLGK		14.2	396.7	491.3
OCT2-H	SLPASL*QR		12.1	439.8	678.4
SGLT2-H	GTVGGYFL*AGR		17.6	553.0	847.4

DMD Fast Forward. Published on November 3, 2022 as DOI: 10.1124/dmd.122.001038
This article has not been copyedited and formatted. The final version may differ from this version.

Peptide sequences for each transporter and respective transitions detected as doubly charged parent ion (Q1: $[M+2H]^{2+}$) and the singly charged fragment ions (Q3: $[M+H]^{+}$). Multiple reaction monitoring (MRM) retention times and heavy label internal standards (IS) are indicated for each peptide respectively.

Figure 1

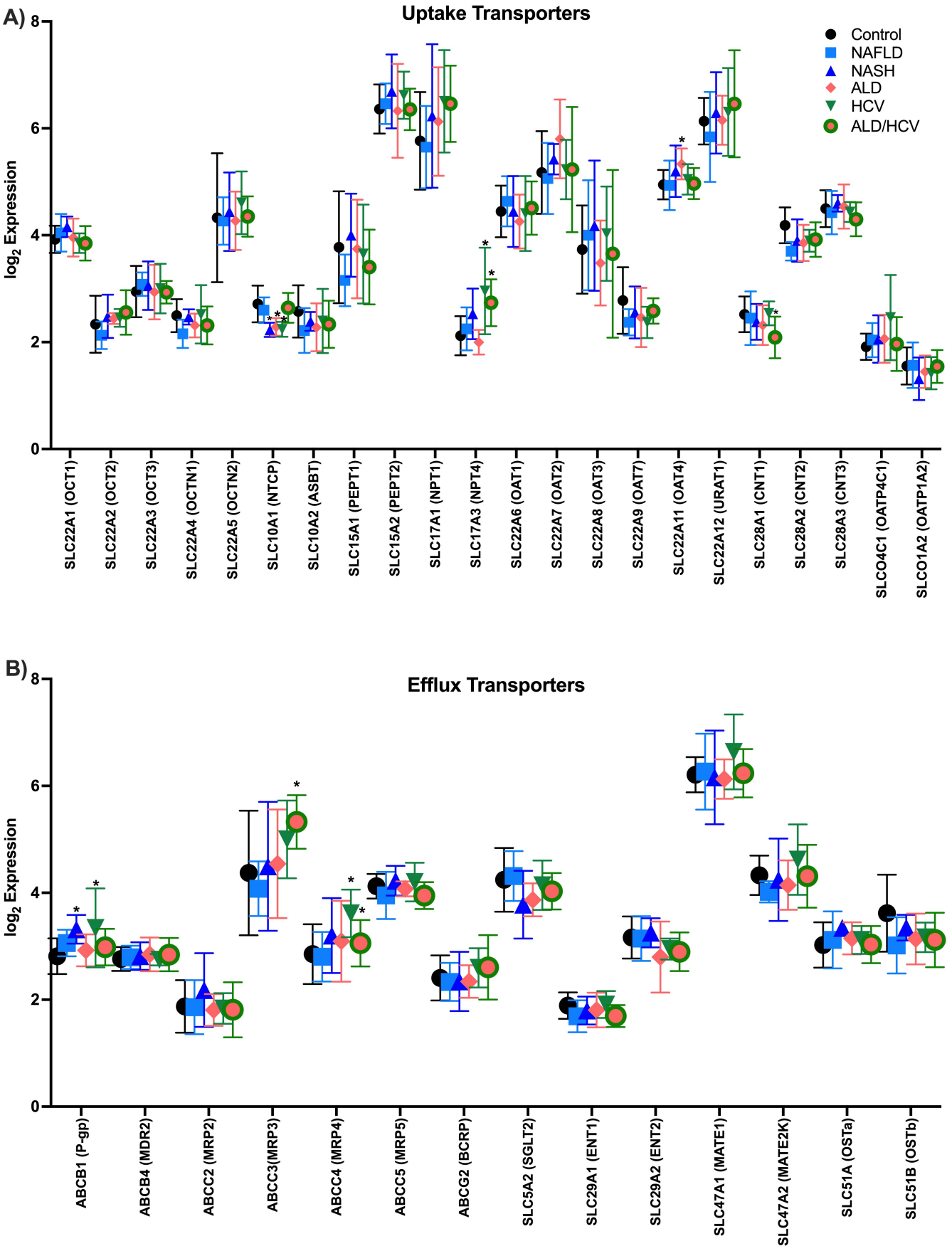
A)
Uptake Transporters
Control
NAFLD
NASH
ALD
HCV
ALD/HCV
log2 Expression
0
2
4
6
8
SLC22A1 (OCT1)
SLC22A2 (OCT2)
SLC22A3 (OCT3)
SLC22A4 (OCTN1)
SLC22A5 (OCTN2)
SLC10A1 (NTCP)
SLC10A2 (ASBT)
SLC15A1 (PEPT1)
SLC15A2 (PEPT2)
SLC17A1 (NPT1)
SLC17A3 (NPT4)
SLC22A6 (OAT1)
SLC22A7 (OAT2)
SLC22A8 (OAT3)
SLC22A9 (OAT7)
SLC22A11 (OAT4)
SLC22A12 (URAT1)
SLC28A1 (CNT1)
SLC28A2 (CNT2)
SLC28A3 (CNT3)
SLCO4C1 (OATP4C1)
SLCO1A2 (OATP1A2)
B)
Efflux Transporters
log2 Expression
0
2
4
6
8
ABCB1 (P-gp)
ABCB4 (MDR2)
ABCC2 (MRP2)
ABCC3(MRP3)
ABCC4 (MRP4)
ABCC5 (MRP5)
ABCG2 (BCRP)
SLC5A2 (SGLT2)
SLC29A1 (ENT1)
SLC29A2 (ENT2)
SLC47A1 (MATE1)
SLC47A2 (MATE2K)
SLC51A (OSTa)
SLC51B (OSTb)

Figure 2

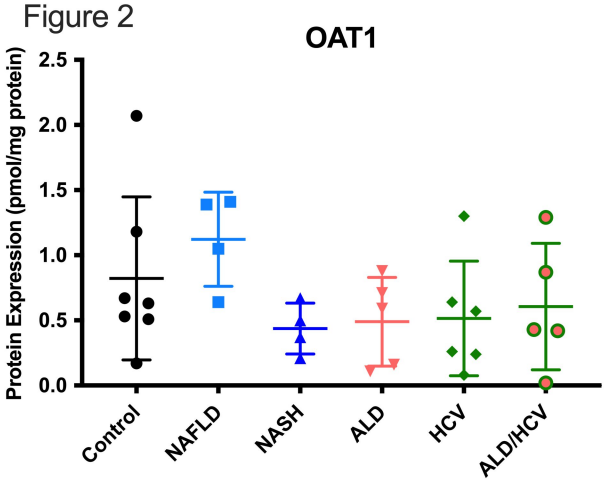
OAT1
Protein Expression (pmol/mg protein)
2.5
2.0
1.5
1.0
0.5
0.0
Control
NAFLD
NASH
ALD
HCV
ALD/HCV

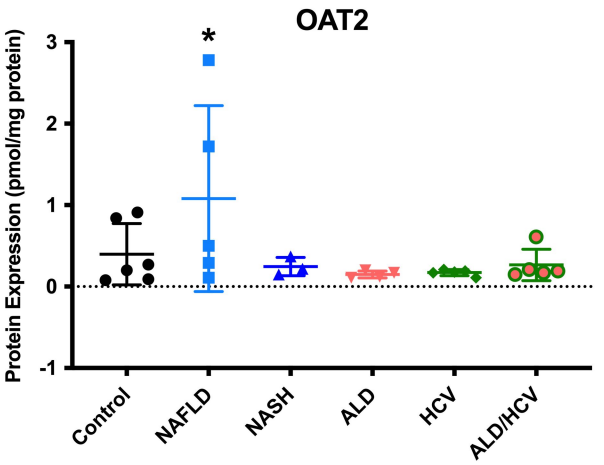
OAT2
Protein Expression (pmol/mg protein)
3
2
1
0
-1
*
Control
NAFLD
NASH
ALD
HCV
ALD/HCV

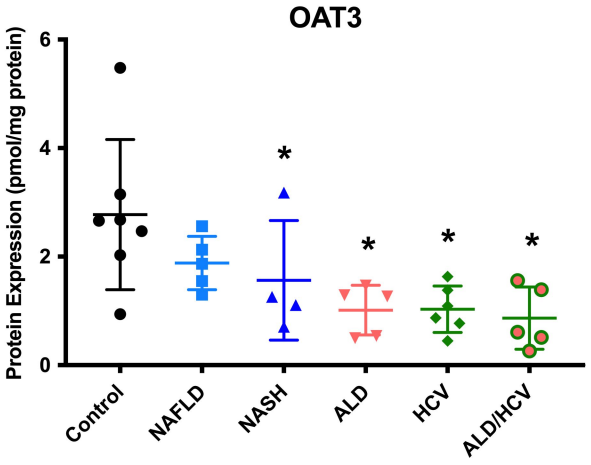
OAT3
Protein Expression (pmol/mg protein)
6
4
2
0
*
*
*
*
Control
NAFLD
NASH
ALD
HCV
ALD/HCV

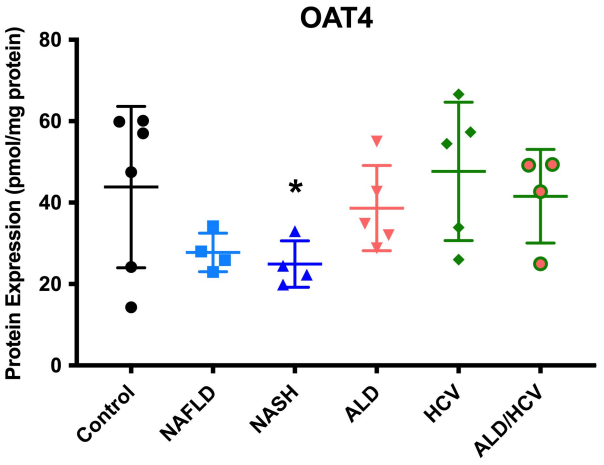
OAT4
Protein Expression (pmol/mg protein)
80
60
40
20
0
*
Control
NAFLD
NASH
ALD
HCV
ALD/HCV

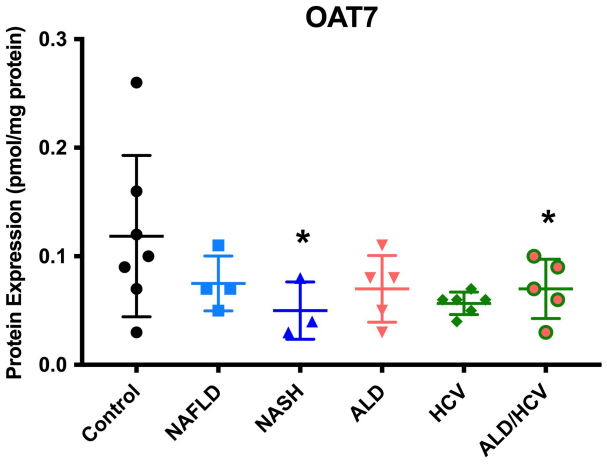
OAT7
Protein Expression (pmol/mg protein)
0.3
0.2
0.1
0.0
*
*
Control
NAFLD
NASH
ALD
HCV
ALD/HCV

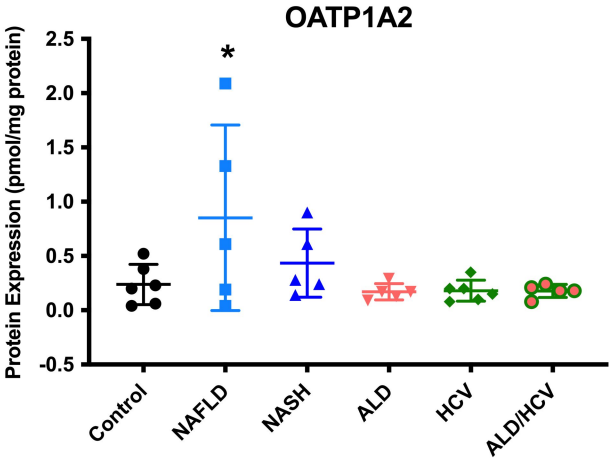
OATP1A2
Protein Expression (pmol/mg protein)
2.5
2.0
1.5
1.0
0.5
0.0
-0.5
*
Control
NAFLD
NASH
ALD
HCV
ALD/HCV

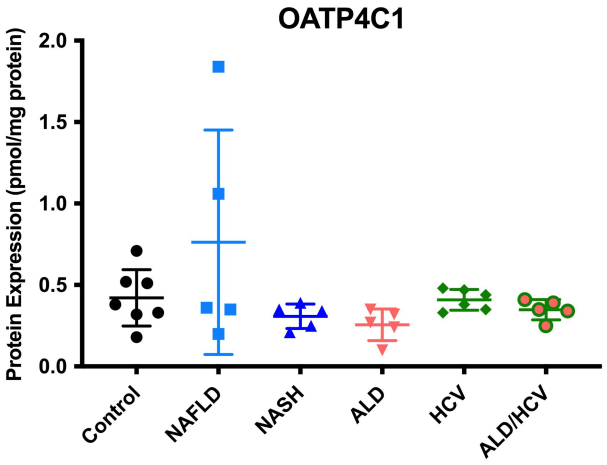
OATP4C1
Protein Expression (pmol/mg protein)
2.0
1.5
1.0
0.5
0.0
Control
NAFLD
NASH
ALD
HCV
ALD/HCV

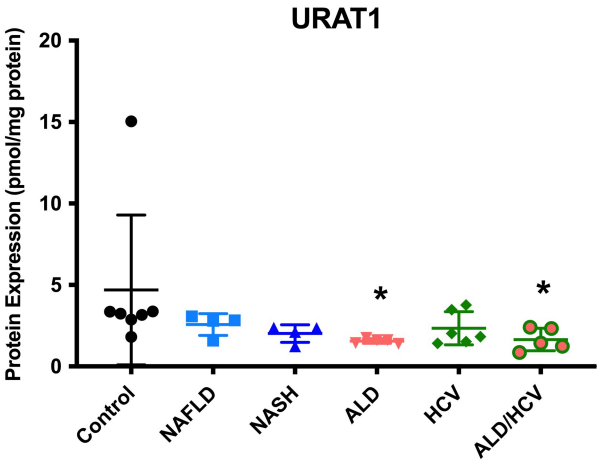
URAT1
Protein Expression (pmol/mg protein)
20
15
10
5
0
*
*
Control
NAFLD
NASH
ALD
HCV
ALD/HCV

Figure 3

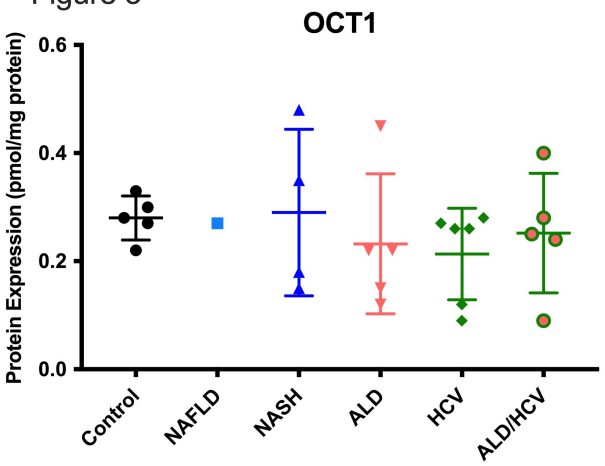
OCT1
Protein Expression (pmol/mg protein)
0.6
0.4
0.2
0.0
Control
NAFLD
NASH
ALD
HCV
ALD/HCV

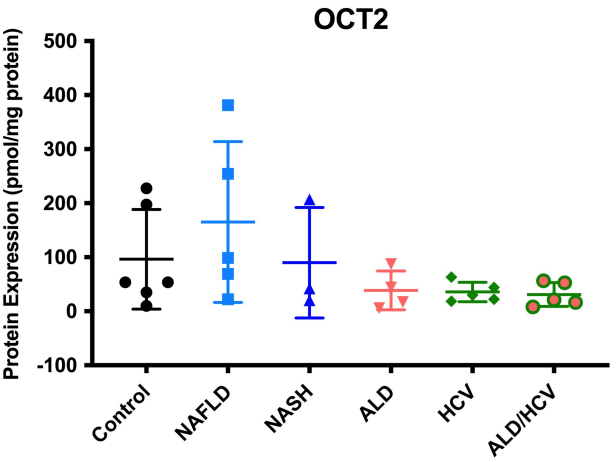
OCT2
Protein Expression (pmol/mg protein)
500
400
300
200
100
0
-100
Control
NAFLD
NASH
ALD
HCV
ALD/HCV

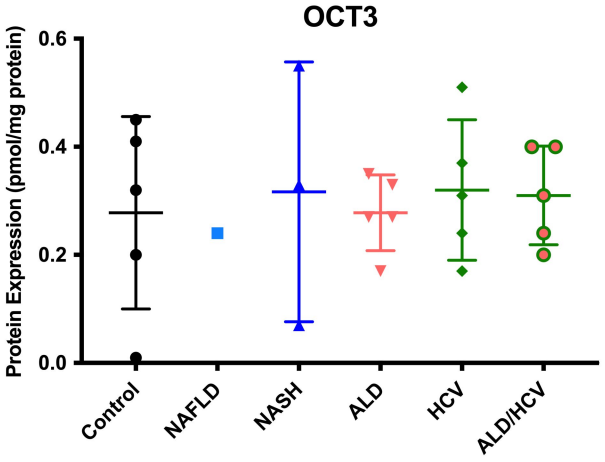
OCT3
Protein Expression (pmol/mg protein)
0.6
0.4
0.2
0.0
Control
NAFLD
NASH
ALD
HCV
ALD/HCV

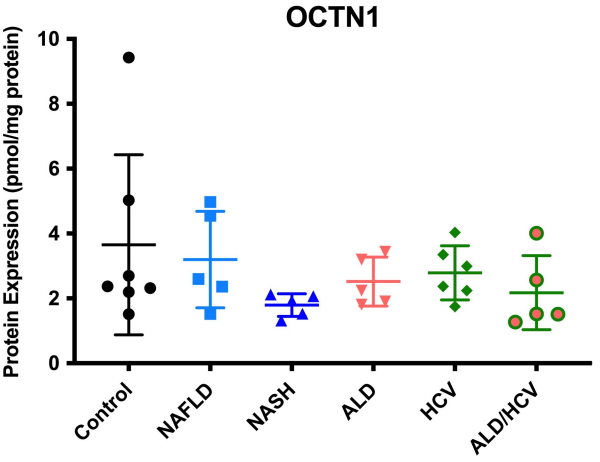
OCTN1
Protein Expression (pmol/mg protein)
10
8
6
4
2
0
Control
NAFLD
NASH
ALD
HCV
ALD/HCV

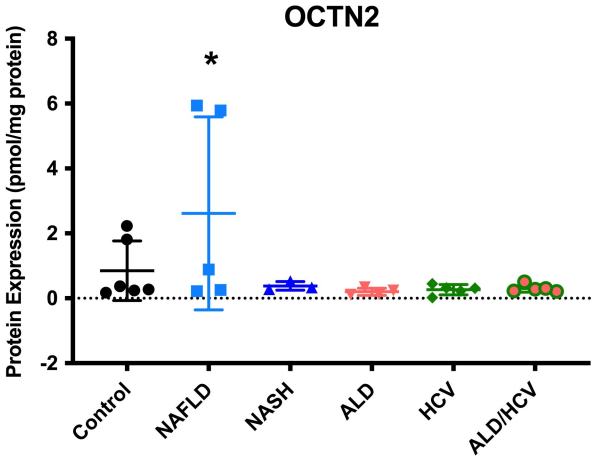
OCTN2
Protein Expression (pmol/mg protein)
*
8
6
4
2
0
-2
Control
NAFLD
NASH
ALD
HCV
ALD/HCV

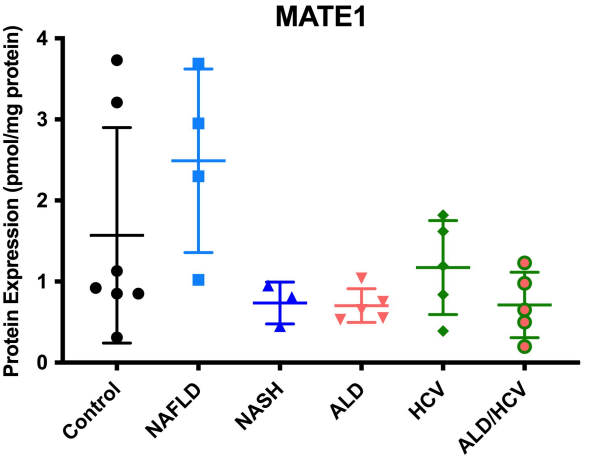
MATE1
Protein Expression (pmol/mg protein)
4
3
2
1
0
Control
NAFLD
NASH
ALD
HCV
ALD/HCV

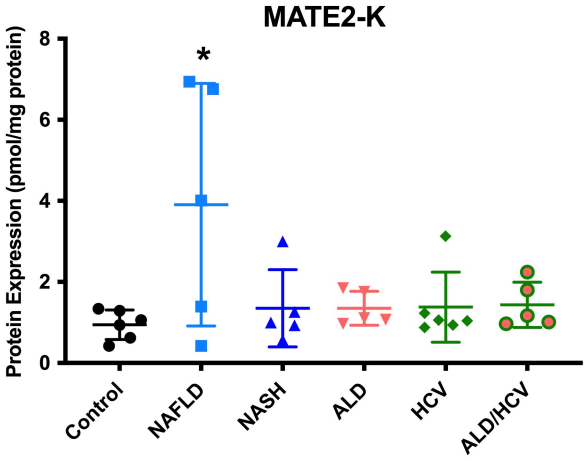
MATE2-K
Protein Expression (pmol/mg protein)
*
8
6
4
2
0
Control
NAFLD
NASH
ALD
HCV
ALD/HCV

Figure 4

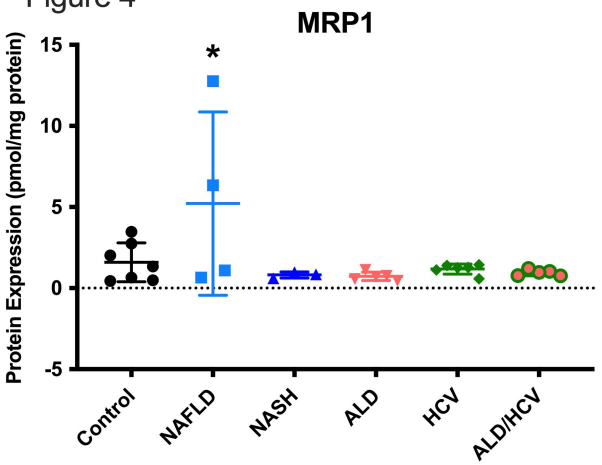
MRP1
Protein Expression (pmol/mg protein)
15
10
5
0
-5
*
Control
NAFLD
NASH
ALD
HCV
ALD/HCV

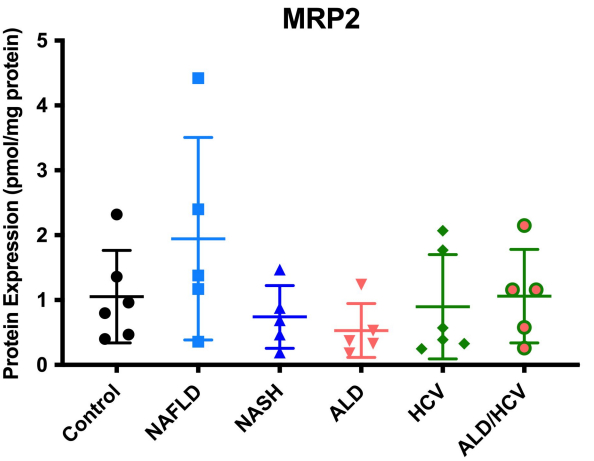
MRP2
Protein Expression (pmol/mg protein)
5
4
3
2
1
0
Control
NAFLD
NASH
ALD
HCV
ALD/HCV

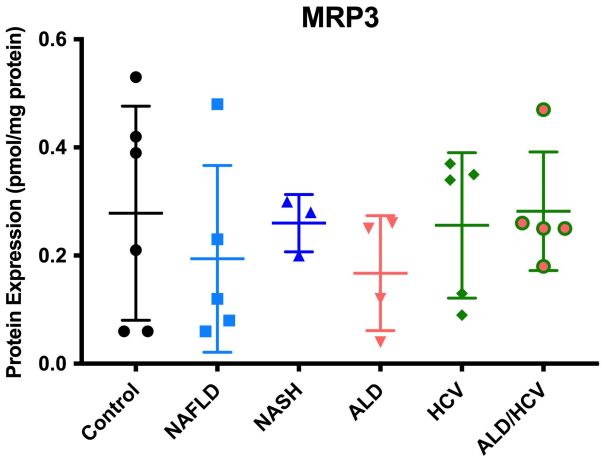
MRP3
Protein Expression (pmol/mg protein)
0.6
0.4
0.2
0.0
Control
NAFLD
NASH
ALD
HCV
ALD/HCV

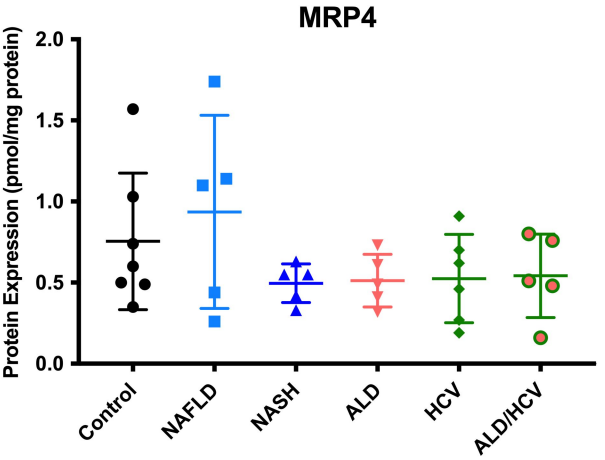
MRP4
Protein Expression (pmol/mg protein)
2.0
1.5
1.0
0.5
0.0
Control
NAFLD
NASH
ALD
HCV
ALD/HCV

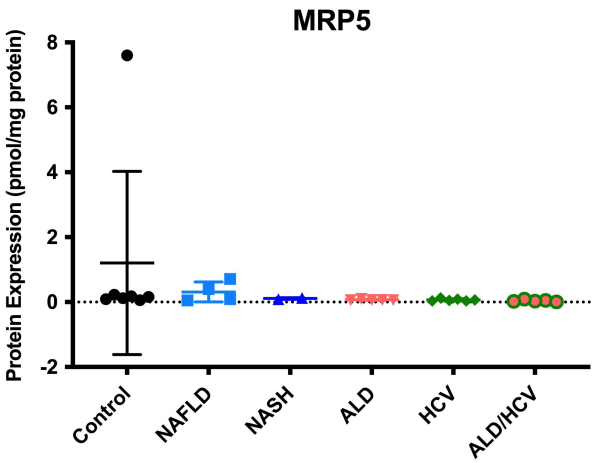
MRP5
Protein Expression (pmol/mg protein)
8
6
4
2
0
-2
Control
NAFLD
NASH
ALD
HCV
ALD/HCV

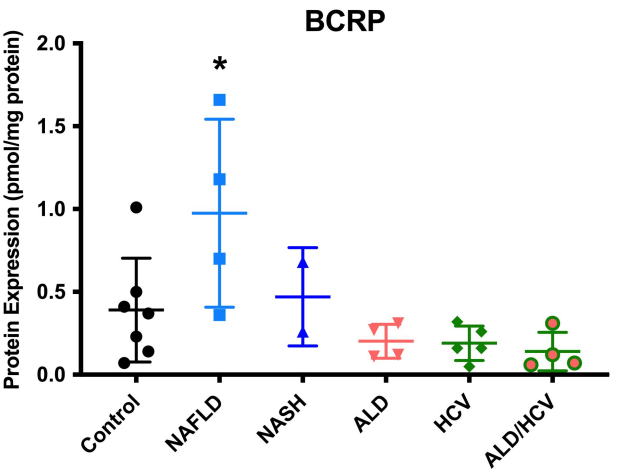
BCRP
Protein Expression (pmol/mg protein)
2.0
1.5
1.0
0.5
0.0
*
Control
NAFLD
NASH
ALD
HCV
ALD/HCV

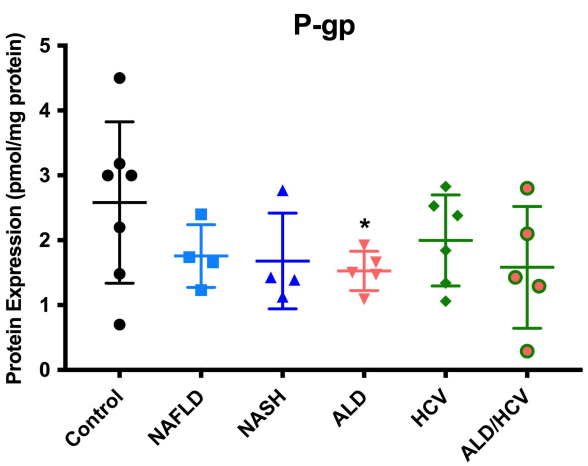
P-gp
Protein Expression (pmol/mg protein)
5
4
3
2
1
0
*
Control
NAFLD
NASH
ALD
HCV
ALD/HCV

Figure 5

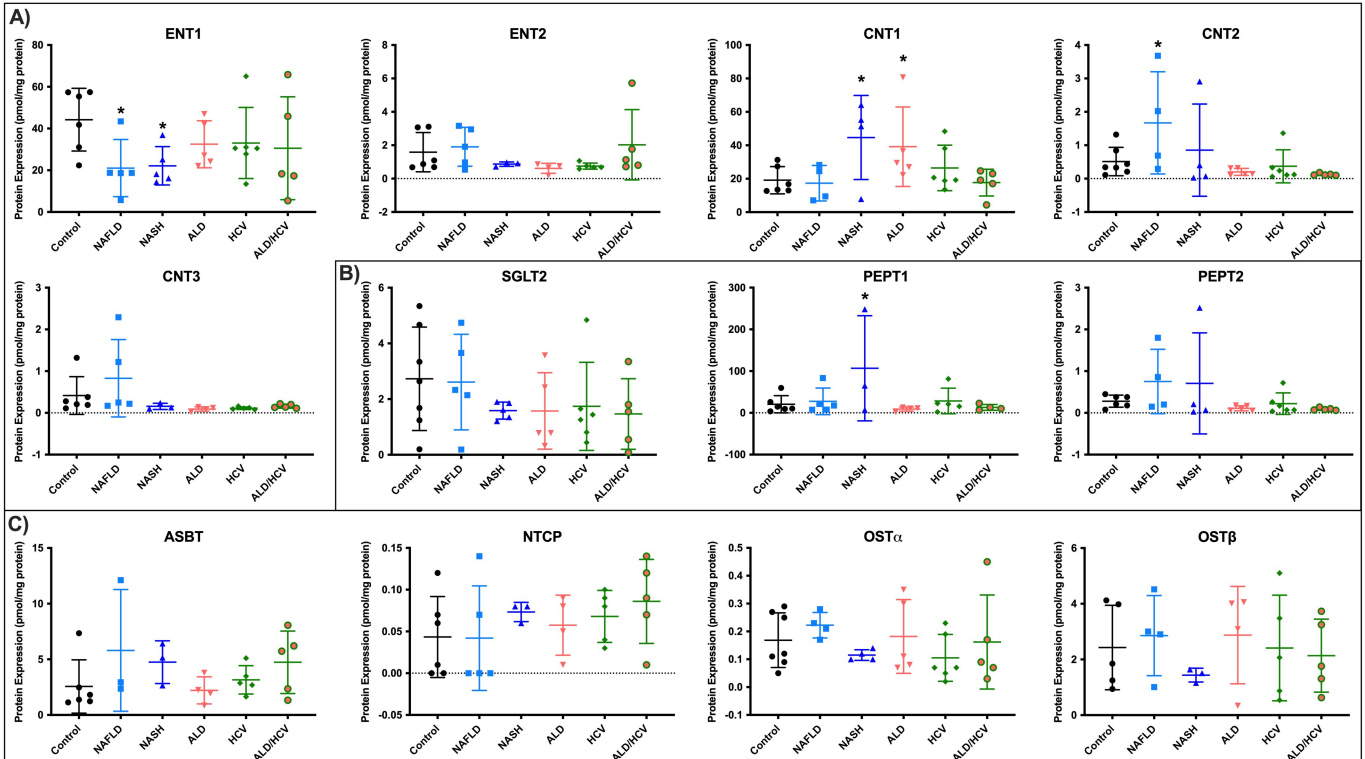
A)
ENT1
ENT2
CNT1
CNT2
CNT3
B)
SGLT2
PEPT1
PEPT2
C)
ASBT
NTCP
OSTα
OSTβ
Protein Expression (pmol/mg protein)
Control
NAFLD
NASH
ALD
HCV
ALD/HCV